Phase Locking, Amplification, and Mode Selection in an 85 GHz Quasioptical Gyroklystron

R. P. Fischer, A. W. Fliflet, and W. M. Manheimer
Plasma Physics Division, Naval Research Laboratory, Washington, D.C. 20375

B. Levush, T. M. Antonsen, Jr., and V. L. Granatstein
Laboratory for Plasma Research and Electrical Engineering Department, University of Maryland, College Park, Maryland 20742

(Received 22 November 1993; revised manuscript received 11 March 1994)

A highly overmoded 85 GHz gyroklystron experiment is reported using two quasioptical resonators. Phase locking at 70 kW output power and 16% efficiency is demonstrated over the entire linewidth of the output resonator by prebunching the electron beam. Amplifier operation at 30 kW output power is observed with over 18 dB gain. Two techniques, mode priming and alpha priming, allow access to the hard excitation region of the gyroklystron. Good agreement is obtained between the multimode simulation code and important features of the experiment.

PACS numbers: 42.52.+x, 85.10.Jz

Gyrotron oscillators operating at millimeter wavelengths have been developed at laboratories worldwide for heating and current drive in magnetic fusion plasmas, where impressive powers and efficiencies have been achieved [1,2]. There are a number of applications where precise frequency and phase control of the rf signals are required, including millimeter-wave radar, atmospheric sensing, drivers for linear accelerators, and deep space communications. A high power gyroklystron operating as an amplifier or a phase-locked oscillator would be attractive for these types of applications. Gyroklystrons operating at microwave frequencies have recently been developed as phase-locked oscillators [3] and efficient high power amplifiers [4]. However, gyroklystrons operating at millimeter wavelengths have been slow to develop due to technical difficulties such as spurious oscillations in the cavities and drift region and velocity spread of the electron beam.

This Letter presents new experimental amplifier, phase-locked oscillator, and mode-primed oscillator results from a proof-of-principle 85 GHz gyroklystron using quasioptical resonators. A detailed comparison is made between the experimental results and a time dependent, multimode simulation code. There are several technical advantages in using quasioptical resonators [5–8], as opposed to conventional cylindrical cavities, in a gyroklystron. First, a high degree of isolation is achieved in this configuration since the resonators are oriented perpendicular to the axis of the electron beam, which minimizes unwanted rf feedback. Second, higher-order transverse modes are eliminated due to the finite size of the resonator mirrors so that excitation of spurious modes is avoided. This particular gyroklystron is unique in that the separation between resonators is large (30 radiation wavelengths) and the mode density in the output resonator is quite high ($\Delta f/f = 0.8\%$) so that mode competition and suppression effects are important [9]. Several new capabilities are demonstrated in the present quasioptical gyroklystron experiment. First, phase locking at 70 kW output power and 16% efficiency is achieved over the entire linewidth of the output resonator using modest drive power by prebunching the electron beam in an upstream resonator. Second amplifier operation is realized with over 18 dB gain, 30 kW output power, and 10% efficiency using a reduced electron pitch angle. The output of the gyroklystron is single moded, and two techniques are demonstrated which accomplish longitudinal mode selection and allow access to the hard excitation region of the gyrotron parameter space.

A schematic diagram of the experiment is shown in Fig. 1, where the magnetron injection gun (80 kV, 40 A) is mounted in the fringing field of the main solenoids. The pitch angle of the electrons ($\alpha = \beta_\perp/\beta_\parallel$) is controlled by varying the resistive divider circuit which powers the mod anode of the gun. The output resonator is formed by a pair of spherically shaped mirrors, where the axis of the resonator is tilted by 2° relative to the plane perpendicular to the electron beam axis. This small tilt allows electrons to interact with both even and odd longitudinal modes in the output resonator, which increases the efficiency and operating region of stable, single-mode operation [9]. The low-Q prebunching resonator consists of two mirrors with centered coupling holes with a quality factor $Q = 2000$. The maximum current is limited to 5 A for a pitch angle $\alpha = 1.9$ due to the threshold current of the input resonator. The magnetic field in the prebuncher is 3.5% higher than the field in the output resonator, which minimizes the effect of velocity spread of the beam in the drift region [10]. The long drift region allows for a large bunching parameter ($q \gtrsim 2$) so that the electrons are optimally bunched in gyrophase angle at the entrance of the second resonator.

An 85 GHz extended interaction oscillator (EIO) drives the input resonator and prebunches the beam. The EIO peak power is 1.5 kW, the maximum pulse length is 2 μsec, and the measured frequency drop is 15 MHz during the pulse. A modified laser calorimeter, which preferentially absorbs 85 GHz radiation, is used to measure the

0031-9007/94/72(15)/2395(4)$06.00

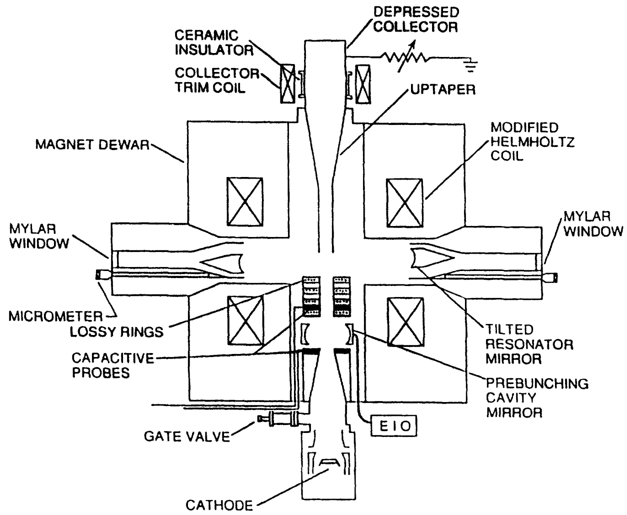

FIG. 1. Schematic of the quasioptical gyroklystron experiment.

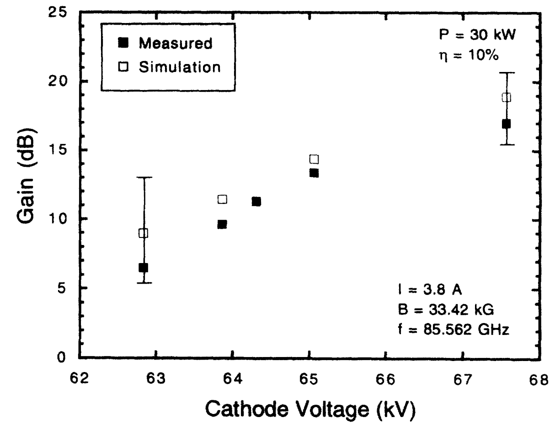

FIG. 2. Measured and simulation amplifier gain versus cathode voltage. The simulation error bars represent a $\pm 10\%$ uncertainty in pitch angle.

average output power from one side of the experiment. The calorimeter is calibrated using both low power cold tests of the surface absorption and 10 W average power tests using the EIO. Time-resolved frequency measurements of the gyroklystron and the EIO are performed using a heterodyne system with a harmonic mixer, a frequency-controlled local oscillator, and bandpass filters. A balanced mixer/phase detector is used to compare the input and output frequencies and detect phase locking. Capacitive probes in the drift region are used to measure the longitudinal charge density and average pitch angle of the electron beam [11]. The time-dependent, multimode theoretical model is described in detail elsewhere [12], and includes the effects of the tilted output resonator, the annular electron beam, the finite rise of the beam voltage and perpendicular energy, phase bunching of the electrons, and space charge depression as the electrons traverse the output resonator.

Although the gyroklystron is designed as an oscillator, it can be operated as an amplifier by reducing the current and pitch angle of the electron beam so that the output resonator is below threshold in the absence of an input signal. The measured 2.5 MHz bandwidth of the amplifier is in excellent agreement with calculated and measured values of the quality factor of the output resonator. Measurements from the balanced mixer/phase detector indicate that there is a fixed phase between the input and output signals with zero beat frequency, which is to be expected. Amplifier gain is plotted in Fig. 2 as a function of cathode voltage for a current of 3.8 A and a measured pitch angle of $\alpha = (0.9\text{–}1.1) \pm 15\%$ over this range of cathode voltage. Peak gains of over 18 ± 1 dB are measured, corresponding to 30 kW output power and an efficiency of 10%. The simulations are performed using the measured values of α with corresponding bunching parameters $q = 1.18\text{–}1.53$. The agreement between the measured and theoretical amplifier gain is quite good, where the simulation error bars represent a $\pm 10\%$ uncertainty in α. Linear theory calculations yield gain values of approximately 20 dB for the parameters in the experiment. For cathode voltages greater than 68 kV, free oscillations occur in the output resonator after the 2 μsec drive pulse is turned off. Significantly higher gains and output powers are possible if the drive and gyrotron voltage pulses fall simultaneously. The gain measurements indicate that the phase bunching of the electrons is preserved over the long drift region, although no attempt has been made to reduce the velocity spread of the beam in the experiment. This is estimated as $\Delta\alpha = \pm(10\text{–}20)\%$ from electron trajectory simulations.

With no prebunching, the minimum beat frequency between the two free-running sources is seen in Fig. 3(a), where the frequency drop of the EIO during the 2 μsec pulse is observed. Application of the EIO signal to the prebunching resonator is shown in Fig. 3(b), where the flat portion of the balanced mixer signal represents the phase-locking bandwidth. Varying the phase shifter in one arm of the diagnostic circuit indicates that there is a fixed phase between the input and output signals and that the relative phase varies from $\pi/2$ to $-\pi/2$ over the locking bandwidth.

The fractional phase-locking bandwidth is plotted in Fig. 4 as a function of drive power to the input resonator. The gyroklystron is operating at an output power of 60 kW with 16% efficiency and a measured pitch angle $\alpha = 1.8$. The input power required to phase lock the gyroklystron is 21 dB less than Adler's relation for direct injection [13], and demonstrates the benefit of prebunching the electron beam [14,15]. The measured phase-locking bandwidth is somewhat larger than the resonance width of the output resonator, which is consistent with gyroklystron operation at moderate efficiency [16]. Operation at optimum detuning and peak efficiency typically yield locking bandwidths of $\frac{1}{2}$ the output resonator bandwidth [17].

Under normal operating conditions with no prebunch-

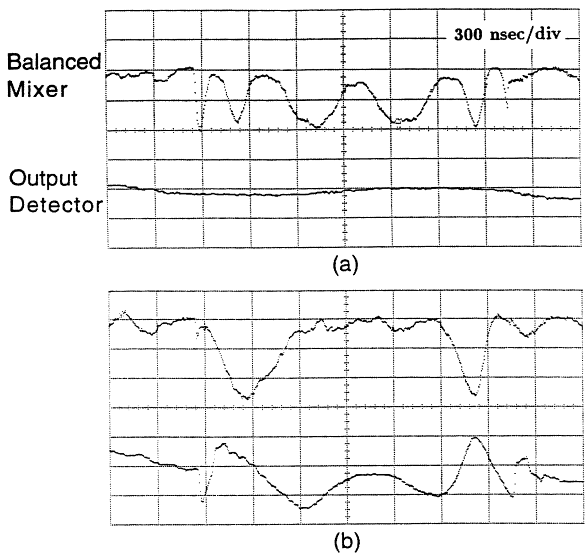

FIG. 3. Balanced mixer traces showing the beat frequency between the gyroklystron and the EIO (a) without prebunching and (b) with prebunching. The flat portion of the trace in (b) represents the phase-locking bandwidth.

ing signal, the output of the gyroklystron is single moded with a peak efficiency of 13%. The measured pitch angle of the electrons is typically $\alpha = 1.9$, resulting in a rather long normalized interaction length ($\mu = 19.5$). Two techniques have been demonstrated which increase the frequency detuning ($\Delta\omega/\omega = 1 - \Omega/\gamma\omega$) and efficiency of the operating mode. The first, mode priming [18], uses electron beam prebunching at 85.5 GHz during the rise of the voltage pulse to select the desired mode in the output resonator. The second technique, alpha priming, rapidly ramps the beam α during the rise of the voltage pulse to excite a higher-frequency longitudinal mode. Both of these methods result in stable, single-mode operation of the gyroklystron at higher detuning and efficiency than is possible for the free running oscillator under normal operating conditions.

Figure 5(a) plots measured and simulation interaction efficiency as a function of normalized detuning $\delta = (r_0/v_\parallel)(\omega - \Omega/\gamma)$ for gyroklystron operation with and without mode priming. Here r_0 is the output radiation waist and $v_\parallel$ is the longitudinal velocity of the electrons. Mode priming is simulated by prebunching the electrons in gyrophase angle with a bunching parameter $q = 2$ for 2 μsec immediately before the flattop of the voltage pulse. The peak α in the simulations is limited to 1.6 to ensure single-mode operation, which is always observed in the experiment. Free-running oscillator operation in the desired 85.5 GHz mode results in relatively low efficiency over a limited range of frequency detunings. Mode priming allows for higher detuning and efficiency, where $\delta > 3.0$ corresponds to the hard excitation region of the gyroklystron [12]. In this region, the operating current is below the start oscillation current of the 85.5 GHz mode

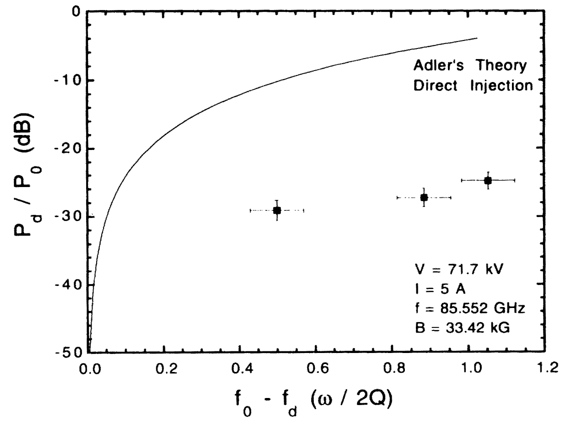

FIG. 4. Gyroklystron phase-locking bandwidth as a function of input drive power.

($I < I_{st}$) and the maximum efficiency is obtained. The multimode simulation code correctly predicts the detuning range for operation with no priming as well as the detuning limits for mode priming. Note that it is possible to mode prime the gyroklystron to operate at detunings and efficiencies which are less than the free-running oscillator. Attempts to increase the detuning to $\delta > 4.0$ result in mode competition with lower-frequency longitudinal modes in both the experiment and the simulations. Peak experimental efficiencies are approximately $\frac{1}{3}$ less than the simulation values, although it is unlikely that this discrepancy is due to insufficient frequency detuning in the experiment. Recent measurements on an identical electron gun indicate that the velocity spread is 2–3 times larger than electron trajectory simulations, which is sufficient to account for the reduced efficiency in cavity gyrotrons [19]. Other effects not included in the theory include second harmonic radiation in the output resonator and the observed sensitivity to mirror alignment.

A similar plot of efficiency versus frequency detuning is given in Fig. 5(b) for oscillator operation with and without alpha priming. This new technique is modeled in the simulation using a voltage rise time of 4.15 μsec and a shorter rise for $\beta_\perp$ of 3.75 μsec. Alpha priming is accomplished in the experiment by slightly reducing the capacitance between the cathode and mod anode in the resistive divider circuit. Note that alpha priming depends only upon the rise of the beam parameters and does not involve the prebunching resonator. A peak efficiency of $(20 \pm 1)\%$ is measured using this new technique, corresponding to an electronic efficiency of 22%, which accounts for Ohmic losses in the output resonator. Alpha priming allows for operation at higher efficiency and detuning by exciting a high-frequency longitudinal mode early in the pulse when competing modes are relatively small. Theoretical efficiencies using alpha priming are essentially identical to those obtained in the mode priming simulations. Good agreement is obtained between the experiment and the simulations for the detuning limits for

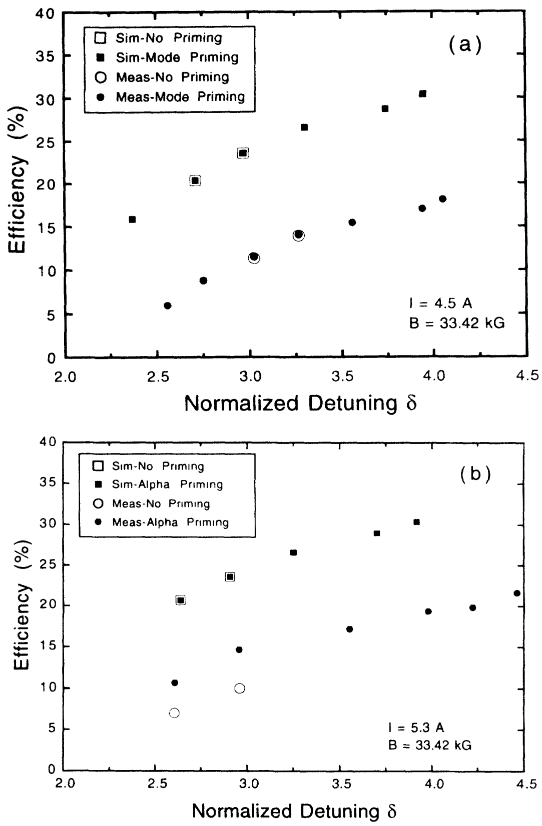

FIG. 5. Measured and simulation efficiency versus normalized detuning δ for (a) mode priming and (b) alpha priming. Mode priming is accomplished using electron beam prebunching, while alpha priming requires variation of the beam α during the rise of the voltage pulse.

alpha-primed operation, although the measured efficiency remains $\sim \frac{1}{3}$ less than the calculated values.

In summary, a quasioptical gyroklystron experiment has been performed which demonstrates several new capabilities as a high power millimeter-wave source. Phase-locked oscillator operation at 70 kW output power and 16% efficiency is realized by prebunching the electron beam in an upstream resonator. The drive power is 21 dB less than that required for direct injection, and the gyroklystron is phase locked over the entire linewidth of the output resonator for large values of frequency detuning. Amplifier operation is demonstrated with over 18 dB gain, 10 kW output power, and 10% efficiency using a reduced pitch angle $\alpha = 1.0$. Two techniques have been identified which allow access to the hard excitation region of the gyroklystron. Mode priming uses electron beam prebunching to preferentially excite the desired mode during the rise of the voltage pulse. Large frequency detunings and efficiencies are also obtained with alpha priming, where the beam α arises somewhat faster than the beam energy. Both of these phenomena are observed in the time-dependent, multimode computer simulations. Stable, single-mode operation is observed at the highest powers and efficiencies, which demonstrates the benefit of tilting the output resonator. The present device can be scaled to higher peak and average power by increasing the beam current and varying the quality factor of the input and output resonators.

We thank G. S. Nusinovich for helpful discussions. This work is supported by the Office of Naval Research and the Department of Energy.

[1] K. E. Kreischer and R. J. Temkin, Phys. Rev. Lett. **59**, 547 (1987).
[2] J. Neilson *et al.*, Proc. SPIE Int. Soc. Opt. Eng. **1576**, 120 (1991).
[3] A. H. McCurdy *et al.*, Phys. Rev. Lett. **57**, 2379 (1986).
[4] W. Lawson *et al.*, Phys. Rev. Lett. **67**, 520 (1991).
[5] A. Bondeson, W. M. Manheimer, and E. Ott, Phys. Fluids **26**, 285 (1983).
[6] P. Sprangle, J. L. Vomvoridis, and W. M. Manheimer, Phys. Rev. A **23**, 3127 (1981).
[7] S. Alberti *et al.*, Phys. Fluids B **2**, 1654 (1990).
[8] A. W. Fliflet, R. P. Fischer, and W. M. Manheimer, Phys. Fluids B **5**, 2682 (1993).
[9] T. M. Antonsen, Jr., B. Levush, and W. M. Manheimer, Phys. Fluids B **2**, 419 (1990).
[10] B. Levush *et al.*, Int. J. Electron. **54**, 749 (1983).
[11] W. C. Guss *et al.*, J. Appl. Phys. **69**, 3789 (1991).
[12] B. Levush and T. M. Antonsen, Jr., IEEE Trans. Plasma Sci. **18**, 260 (1990).
[13] R. Adler, Proc. IRE **34**, 351 (1946).
[14] V. S. Ergakov and M. A. Moiseev, Radiophys. Quantum Electron. **18**, 89 (1975).
[15] A. W. Fliflet and W. M. Manheimer, Phys. Rev. A **39**, 3432 (1989); W. M. Manheimer, Int. J. Electron. **63**, 29 (1987).
[16] I. G. Zarnitsyna and G. S. Nusinovich, Radiophys. Quantum Electron. **18**, 339 (1975).
[17] W. M. Manheimer, B. Levush, and T. M. Antonsen, Jr., IEEE Trans. Plasma Sci. **18**, 350 (1990).
[18] A. H. McCurdy and C. M. Armstrong, Phys. Fluids B **3**, 212 (1991).
[19] W. C. Guss *et al.* (to be published).